polymers

Article

FRP-RC Beam in Shear: Mechanical Model and Assessment Procedure for Pseudo-Ductile Behavior

Floriana Petrone * and Giorgio Monti

Department of Structural and Geotechnical Engineering, Sapienza University of Rome,
via A. Gramsci 53, 00197 Roma, Italy; E-Mail: giorgio.monti@uniroma1.it

* Author to whom correspondence should be addressed; E-Mail: floriana.petrone@uniroma1.it;
Tel.: +39-06-4991-9184; Fax: +39-06-4991-9192.

Abstract: This work deals with the development of a mechanics-based shear model for reinforced concrete (RC) elements strengthened in shear with fiber-reinforced polymer (FRP) and a design/assessment procedure capable of predicting the failure sequence of resisting elements: the yielding of existing transverse steel ties and the debonding of FRP sheets/strips, while checking the corresponding compressive stress in concrete. The research aims at the definition of an accurate capacity equation, consistent with the requirement of the pseudo-ductile shear behavior of structural elements, that is, transverse steel ties yield before FRP debonding and concrete crushing. For the purpose of validating the proposed model, an extended parametric study and a comparison against experimental results have been conducted: it is proven that the common accepted rule of assuming the shear capacity of RC members strengthened in shear with FRP as the sum of the maximum contribution of both FRP and stirrups can lead to an unsafe overestimation of the shear capacity. This issue has been pointed out by some authors, when comparing experimental shear capacity values with the theoretical ones, but without giving a convincing explanation of that. In this sense, the proposed model represents also a valid instrument to better understand the mechanical behavior of FRP-RC beams in shear and to calculate their actual shear capacity.

Keywords: mechanics-based shear model; actual shear capacity of fiber-reinforced polymer reinforced concrete (FRP-RC) beams; contribution of stirrups

1. Introduction

Shear capacity equations proposed by current codes for fiber-reinforced polymer reinforced concrete (FRP-RC) elements stem either from regression-based models, derived from experimental results available in the literature, or from simplified strut-and-tie models with an implicit application of the plasticity theory. None of these formulations is based on mechanical models that aim at capturing the real contributions of all resisting mechanisms to the shear capacity. Formulations belonging to the first group, e.g., ACI 318-08 [1], give the shear strength as the sum of the maximum contributions of all resisting elements—FRP, stirrups and concrete—while in the second group, e.g., CNR-DT200 [2], it equals the minimum value between the maximum concrete strength and the sum of FRP and stirrup maximum strengths.

Both approaches, beyond not being rigorous, can lead to overestimating of the shear strength of FRP-strengthened RC elements.

The lack of a mechanical model able to correctly render the interaction between FRP and steel shear reinforcement has been highlighted several times when dealing with the analysis of parameters that affect the shear behavior of FRP-strengthened RC structures.

To this end, Lima and Barros [3], working on a large database of experimental results collected from the literature, conducted a comparative study aiming at assessing the reliability of the most common shear design models: after comparing the experimental results with the theoretical values, it was pointed out that, in most cases, current equations overestimate the experimentally measured shear capacity.

As a matter of fact, in the last two decades, most research efforts have been devoted to defining the contribution of FRP to shear capacity, however, without developing a comprehensive mechanical model capable of accounting for the interaction of all resisting mechanisms. In this framework, Khalifa *et al.* [4] proposed two design algorithms to compute the contribution of FRP to the shear capacity of RC flexural members: the first one is based on the evaluation of the effective stress that causes the tensile fracture of FRP sheets and the second one on the bond mechanism. However, the overall shear capacity is still expressed as the sum of the contribution of all resisting mechanisms. Triantafillou and Antonopoulos [5] introduced a design model to evaluate the contribution of FRP to the shear capacity: it is based on the calculation of an effective FRP strain, obtained through calibration with experimental tests and defined as the minimum value among the maximum strain to control the crack opening, the strain corresponding to premature shear failure due to FRP debonding and the strain corresponding to shear failure combined with or followed by FRP tensile fracture. Along this line of research, many models have been proposed, Chen and Teng [6], Carolin and Taljsten [7] and Monti and Liotta [8], with the latter having the merit of expressing the FRP effective stress through a closed-form equation obtained from a mechanics-based analytical model: after the constitutive law of an FRP layer bonded to concrete is defined, the compatibility condition is imposed by the shear crack opening, and then, analytical expressions of the stress field in FRP strips/sheets crossing a shear crack are derived.

Chaallal *et al.* [9] proposed an equation to evaluate the effective strain of FRP based on the total shear-reinforcement ratio $\rho_{tot} = n \cdot \rho_f + \rho_s$, which yields promising results for a limited range of shear-reinforcement values.

Pellegrino and Modena [10] presented an analytical model to describe the shear capacity of RC beams that takes into account the interaction between stirrups and FRP: starting from the assumption that the FRP strain equals the stirrups' strain, the FRP contribution to the shear capacity is obtained by imposing the equilibrium condition between concrete and FRP at failure. The model is based on a weak compatibility condition, since a rough assumption about the strain of all of the stirrups is made: in fact, to account for the unknown value of the stress and strain of all of the stirrups crossing the crack, a reduction coefficient $\alpha = 0.75$ is introduced. Bukhari *et al.* [11] presented a detailed review of the models proposed by current codes—ACI 2008 and Eurocode 2 [1,12]—pointing out that the shear strength so calculated does not match the values of experimental results when considering varied typologies—mechanical and geometrical properties—of structural elements. Even if some limits of the current design approaches are analyzed and the importance of the interaction between steel and FRP is highlighted, a design approach is not proposed. Modifi and Chaallal [13], after examining all of the parameters that mainly influence the shear behavior of FRP-strengthened RC members and reviewing the role of these parameters in current design codes, suggested a new design method to account for the effect of transverse steel by introducing a cracking modification factor β_c, evaluated as a function of the geometrical ratio of steel and FRP and the respective Young's moduli.

The approach presented hereafter stems from a mechanical model solved by imposing a strong compatibility condition along the crack between FRP strips/sheets and steel stirrups and an equilibrium condition between tensile and compressive resultant forces. Overall, the proposed model allows predicting the failure sequence of the resisting elements while checking the stress of the concrete strut, but most of all, it allows for a better understanding of the underlying mechanical behavior determining the actual shear resistance of an RC member strengthened in shear with FRP.

2. New Mechanical Model

Starting from the model of Figure 1, which represents the general configuration of an RC cracked beam strengthened in shear with FRP, the simplified model in Figure 2 has been defined in order to fulfill the following requirements: (1) reproducing the real mechanical behavior of the structure, with reference to all of the (compressive and tensile) resisting mechanisms and to their stiffness and resistance, for any possible arrangement of the steel tensile bars and FRP strips/sheets; (2) providing a model that can be the basis for a reliable procedure of the design and verification of structural elements, especially referring to the pseudo-ductile behavior of a beam failing in shear; and (3) putting forward a design/verification methodology able to allow the control of the stress in each resisting element.

Since the geometry of the structure and the mechanical characteristics of the materials are given quantities, the solution of the system can be conveniently carried out by imposing a strong compatibility condition along the crack and the equilibrium condition between the compressive and tensile resultant forces. The compatibility condition allows one to calculate the actual strain of each fiber of FRP and each stirrup crossing the crack, from which the corresponding tensile stress can be easily derived. Once the overall acting tensile force is known, the equilibrium condition gives the corresponding compressive force in the concrete strut, whose magnitude will clearly depend on the geometry of the system.

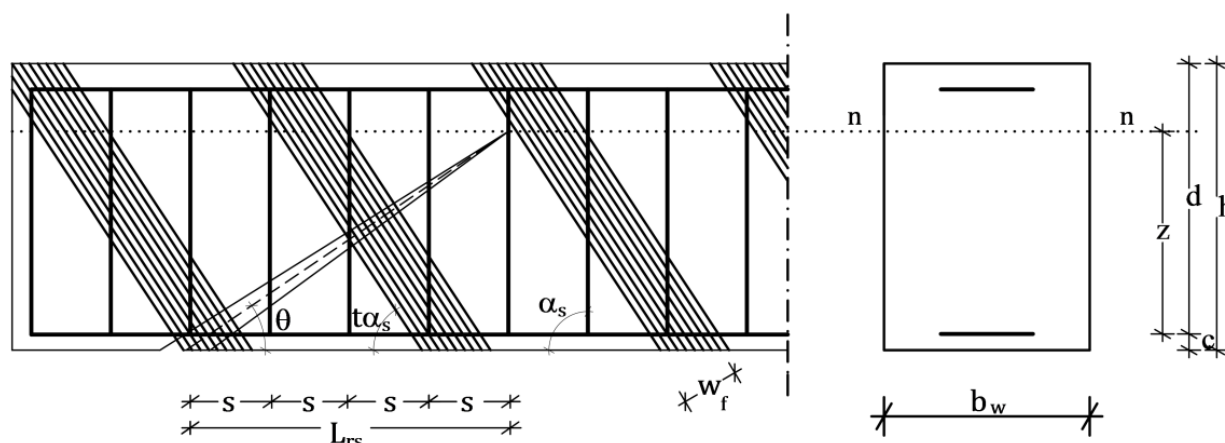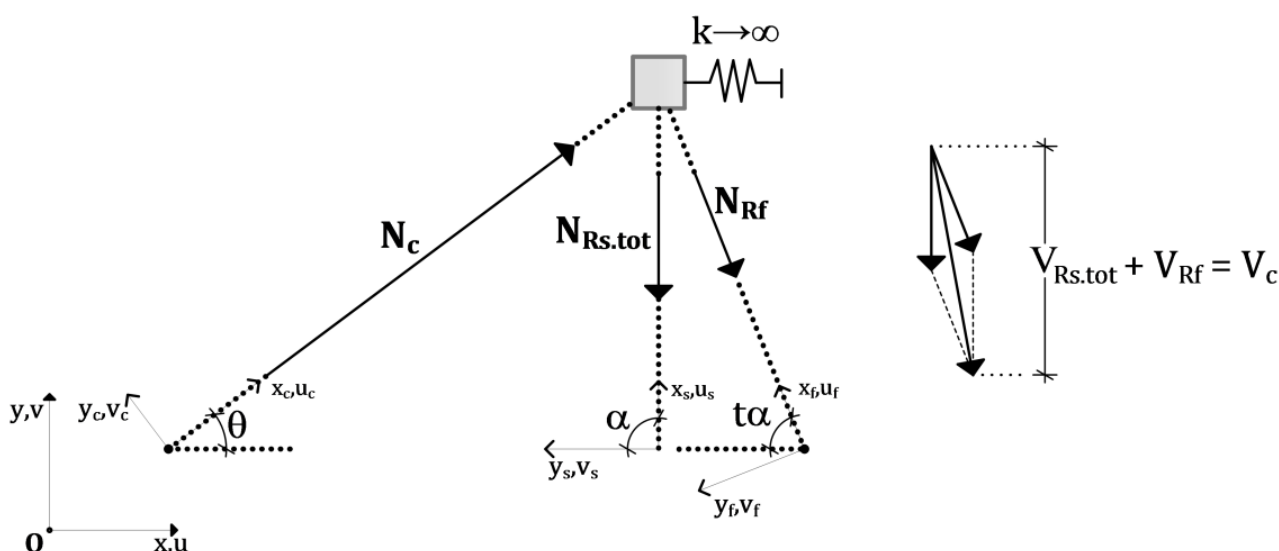**Figure 1.** RC beam strengthened in shear with FRP strips.

Figure 2. Simplified model.

In the following sections, it will be firstly shown how the compatibility condition is set along the crack and how it is employed to calculate stress and strain in the FRP, Monti and Liotta [8] and stirrups, respectively, to derive their actual contribution to the shear capacity. Then, explicitly referring to the simplified mechanical model here proposed, the equilibrium condition is imposed to calculate the stress in the concrete strut.

These three closed form equations expressing the stress of FRP, stirrups and concrete strut as a function of the crack opening γ and the position along the crack x are then employed to solve the mechanical model.

3. Compatibility Condition

Figure 1 shows a typical configuration of a cracked RC beam strengthened in shear with FRP, where two FRP strips and five stirrups cross the crack. At each location along the crack, that is along the x-axis of the local reference system in Figure 3, the strain in the FRP strips and in the stirrups change proportionally to the crack width w_{cr}, which is assumed to vary linearly with x:

$$w_{cr} = 2 \cdot x \tan \frac{\gamma}{2} \qquad (1)$$

where γ is the crack opening angle.

Figure 3. Compatibility along the crack: FRP and stirrup deformation.
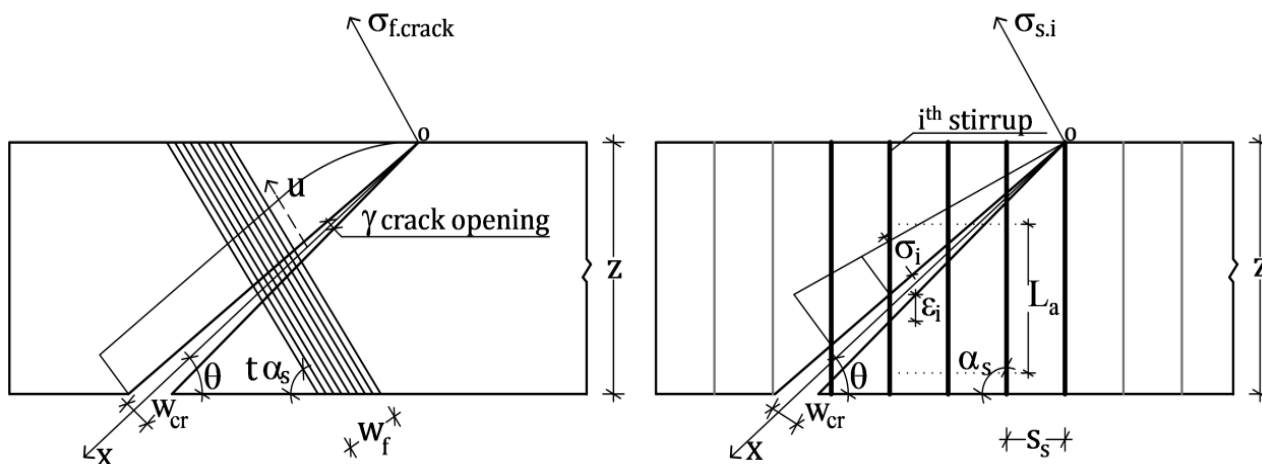
Therefore, within the portion of beam representing the shear mechanical model, the contribution of FRP and steel changes with both x and γ, ensuring that at each location along the crack and for any crack opening, we look at the real contribution of FRP and steel.

According to this condition, in the following, the contribution of FRP and stirrups will be calculated.

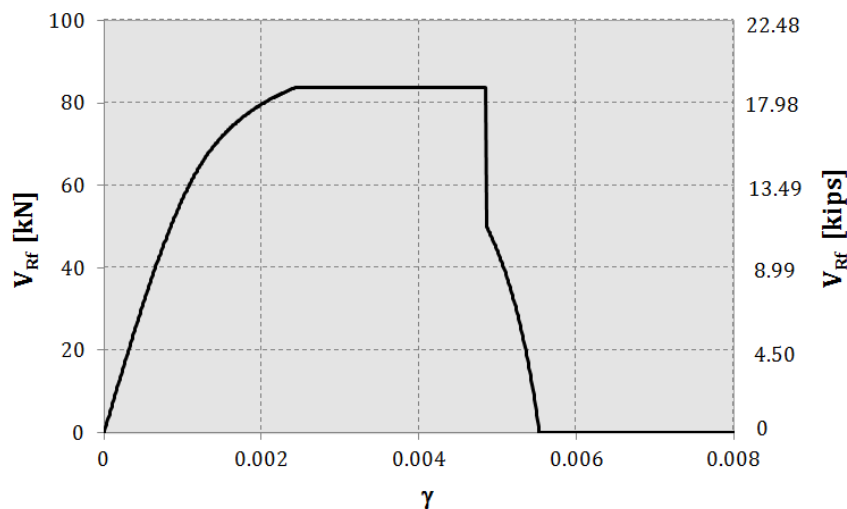## 4. Contribution of FRP to Shear Capacity

The contribution of FRP sheets/strips to the shear capacity can be calculated as follows:

$$V_{Rf}(\gamma, x) = 0.9d \cdot \sigma_{f,eff}(\gamma, x) \cdot 2t_f \left(\cot\theta + \cot t\alpha_s \right) \frac{w_f}{p_f} \qquad (2)$$

where $d = h - c$ is the effective depth of the cross-section, see Figure 1; $\sigma_{f,eff}(\gamma, x)$ is the effective stress in the FRP, expressed as a function of the crack opening γ and the location x, calculated according to the model proposed by Monti and Liotta [8], and θ and $t\alpha_s$ are the slopes of the crack and of the FRP strips/sheets with respect to the beam longitudinal axis, respectively, the latter expressed as a ratio of the slope of the stirrups α_s through the factor t. Moreover, t_f is the thickness of the single FRP sheet/strip, w_f is the FRP sheets/strips width and p_f is the single FRP sheet width: the ratio w_f/p_f can be conveniently read as the number of FRP strips/sheets crossing the crack.

It is worth noticing that when considering a single FRP sheet crossing the crack, which is the case analyzed herein, $V_{Rf}(\gamma, x)$ actually corresponds to $V_{Rf}(\gamma, L_{cr})$, where $L_{cr} = z / \sin\theta$ is the length of the crack (see Figure 1) and is a constant value when a certain geometrical configuration of the beam and θ are assigned. This condition explains why, in Figure 4, we see just one curve representing V_{Rf}, expressed as a function of γ.

Figure 4. Contribution of FRP to the shear capacity on varying of the crack opening γ. Parameters: $H = 400$ mm; $\theta = 30°$; $E_f = 390$ GPa; $t_f = 0.254$ mm; $t = 1$; $R_{ck} = 30$ MPa.

5. Contribution of Stirrups to Shear Capacity

The overall contribution of the stirrups to the shear capacity can be calculated as the sum of the contributions of each single stirrup, based on its effective strain as it is crossed by the crack, as a function of both the crack opening γ and the position x along the crack; see Figure 3. Therefore, the contribution of all of the stirrups to the shear capacity can be expressed as:

$$V_{Rs.tot}(\gamma, x) = \sum_{i=1}^{n} V_{Rs.i}(\gamma, x) \qquad (n = 1, 2 \ldots n_s) \tag{3}$$

where $V_{Rs.i}(\gamma, x)$ is the shear strength of one of the n_s stirrups. Therefore, Equation (3) can also be expressed as:

$$V_{Rs.tot}(\gamma, x) = 0.9 \cdot z \frac{A_{s_1}}{s_s}(\cot \alpha_s + \cot \theta)\sin \alpha_s \sum_{i=1}^{n} \sigma_{s_i}(\gamma, x) \tag{4}$$

where $A_{s_1} = n_b \pi \phi_s^2 / 4$ is the cross-sectional area of one stirrup, n_b is the number of legs of the single stirrup and ϕ_s is the bar diameter; s_s is the spacing of stirrups; $\sigma_{s_i}(\gamma, x) = \min\left[E_s \varepsilon_{s_i}(\gamma, x), f_{ym}\right]$ is the tensile stress in each stirrup that is expressed as a function of the strain ε_{s_i}, given as:

$$\varepsilon_{s_i}(\gamma, x) = \frac{2 \cdot x \tan(\gamma/2)}{\sin(\alpha_s + \theta) \cdot L_a} \tag{5}$$

Where all of the symbols have the meaning explained above and L_a is the "bonding length" of the stirrups. Notice that the numerator of Equation (5) represents the crack width; see the compatibility condition in Equation (1).

Notice that, since the crack width changes along the x-axis by following an assumed linear law, also the strain of each stirrup varies linearly along the longitudinal axis of the crack. Figure 5 shows how strains and stresses of the stirrups change as a function of γ for the case of four stirrups crossing the

crack. For example, when $\gamma = 1 \cdot 10^{-3}$ (see the dotted lines), the first stirrup has zero strain and stress, because it is placed at the crack tip (see Figure 3); the second one is in the linear field and contributes to the shear capacity proportionally to its stress (see Equation (4)); the third and fourth, which are the farthest from the crack tip, give their maximum contribution to the shear capacity, since they are both yielded.

Then, the overall contribution of the stirrups to the shear capacity on the varying of γ is shown in Figure 6, demonstrating that, for the set of variables chosen for this analysis, not all of the stirrups contribute to the shear capacity with their maximum strength: this confirms that the common assumption of assuming all of the stirrups as yielded can lead to an unsafe overestimation of the overall shear capacity.

Figure 5. Strain and stress of each stirrup as a function of the crack opening γ. Parameters: $H = 400$ mm; $\theta = 30°$; $s_s = 100$ mm; $f_{yk} = 355$ MPa; $E_s = 210$ GPa .
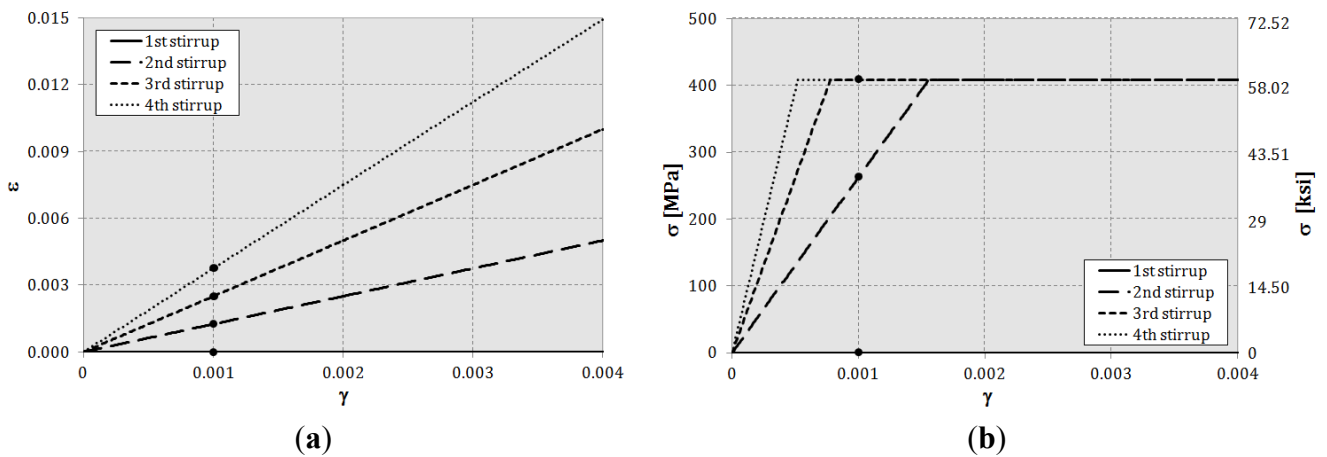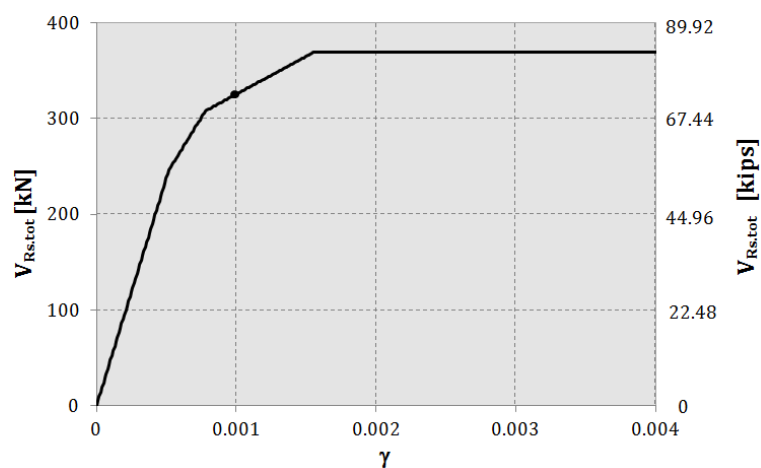

(a)

(b)

**Figure 6.** Overall contribution of stirrups to the shear capacity on varying of γ. Parameters: $H = 400$ mm; $\theta = 30°$; $s_s = 100$ mm; $f_{yk} = 355$ MPa; $E_s = 210$ GPa .

The compatibility condition imposed along the crack allows evaluating the "effective contribution" of FRP sheets/strips and stirrups to the shear capacity on varying of γ, as shown in the following Figure 7.

Figure 7. Variation of $V_{\mathrm{Rs.tot}}(\gamma, x)$ and $V_{\mathrm{Rd.f}}(\gamma)$ on varying of γ. Parameters: $H = 400$ mm; $\theta = 30°$; $s_s = 100$ mm; $f_{yk} = 355$ MPa; $E_s = 210$ GPa; $E_f = 390$ GPa; $t_f = 0.254$ mm; $t = 1$; $R_{ck} = 30$ MPa.
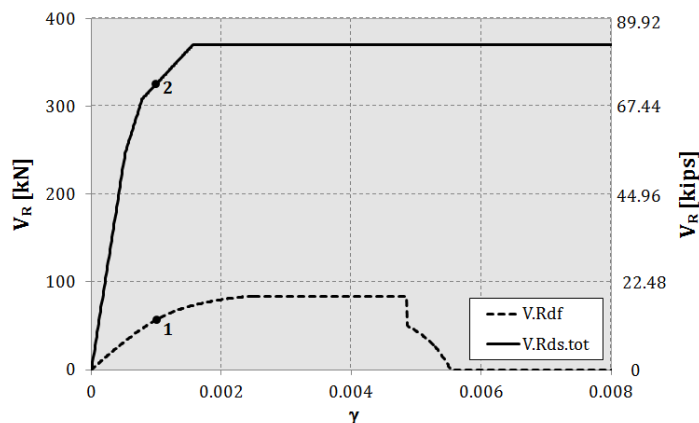
6. Equilibrium Condition: Concrete Strut Crushing

Figure 2 shows the proposed simplified mechanical model where: $N_{\mathrm{Rs.tot}}$ is the axial tensile force acting in all of the stirrups; N_{Rf} is the axial force in the FRP sheet; and N_c is the corresponding axial force in the concrete strut.

The equilibrium of the resultant forces of the simplified model (see Figure 2) reads:

$$V_{\mathrm{Rf}}(\gamma) + V_{\mathrm{Rs.tot}}(\gamma, x) = V_c(\gamma, x) \tag{6}$$

where $V_c(\gamma, x)$ is the vertical projection of the axial force acting on the concrete strut. Therefore, in order for equilibrium to be satisfied, the following condition has to be met:

$$V_c(\gamma, x) \le V_{c,\max} \tag{7}$$

where $V_{c,\max}$ is the vertical component of the strut compression strength. Equation (7) can be made explicit as follows:

$$\sigma_c(\gamma, x) \cdot b_w L_{rs} \sin^2 \theta \le f_c' \cdot b_w L_{rs} \sin^2 \theta \tag{8}$$

where θ and b_w have the meaning explained above and $L_{rs} = z(\cot\theta + \cot\alpha_s)$ represents the length of the representative span of the shear resisting model; see Figure 1. Notice that $f_c' = 0.6 f_c (1 - f_c/250)$ is the reduced compressive strength of concrete, according to Regan [14], which approximately accounts for the biaxial stress state in concrete, by reducing its compressive strength.

Equation (8) can be further simplified into:

$$\sigma_c(\gamma, x) \le f_c' \tag{9}$$

which represents the verification of a concrete section subjected to the axial force $F = V_c(\gamma, x)/\sin\theta$.

7. Parametric Study

For the purpose of validating the model here proposed, a parametric study has been conducted: the variation of the steel stirrup and FRP sheets/strip contribution to the shear capacity at varying of the crack opening γ has been analyzed for different values of the following parameters:

- $H = 400$ mm; 600 mm is the depth of the cross-section;
- $\theta = \pi/6$; $\pi/4$ is the crack slope to the beam longitudinal axis;
- $s = 100$ mm; 200 mm is the stirrup spacing;
- $E_f = 200,000$ MPa ; 390,000 MPa is the Young's modulus of FRP sheets/strips;
- $t_f = 0.127$ mm; 0.22 mm is the thickness of the single FRP sheet/strip;
- $t = 1$; 0.5 is the ratio of FRP to stirrups slopes; see Figure 1 and Figure 3;
- $R_{ck} = 18$ MPa; 30 MPa is the concrete compressive strength.

Among all of the results obtained from the combination of the parameters above, three cases are analyzed in detail thereafter and shown in Figures 8–10: in Plots (a) and (c), long-dotted and solid curves trace the contribution of FRP sheet, V_{Rf}, and steel stirrups, $V_{Rs.tot}$, to the shear capacity, respectively, and short-dotted lines the variation of the compressive axial force in the concrete strut, $N_{c.check}$. Therefore, by drawing a vertical line at any value of the crack opening γ, it is possible to check the failure sequence of the shear resisting elements and the corresponding actual contribution of each of them to the current shear capacity. Plots (b) and (d) also show how many stirrups are intercepted by the crack and how much each of them contributes to the shear capacity at varying of the crack opening γ.

Figure 8a–c shows the case of pseudo-ductile shear behavior, wrongly taken for granted in current design and assessment procedures, meaning that the yielding of stirrups precedes the FRP debonding, and the concrete strut does not crush.

The parameters considered for Cases (a) and (c) are in the following Table 1.

Table 1. Pseudo-ductile shear behavior: parameters.

Case	H (mm)	θ (degrees)	s (mm)	E_f (GPa)	E_s (GPa)	t_f (mm)	t	R_{ck} (MPa)	f_{yk} (MPa)	α_s (degrees)	ϕ_s (mm)
(a)	450	30	200	390	210	0.44	1	20	335	90	8
(c)	400	45	100	200		0.254		30			

Referring to (a), the graph shows that at $\gamma = 0.0015$, the FRP sheet debonds, when all of the stirrups, three in this case, not considering that at the crack tip, see (b), are yielded and the concrete strut is not crushed. Therefore, in this case, along with the one shown in (c) and (d), FRP and stirrups give their maximum contribution to the shear capacity.

Figure 8. Pseudo-ductile shear behavior: (**a**,**c**) the contribution of FRP and stirrups to the shear capacity at varying of γ; (**b**,**d**) the actual contribution of each stirrup at varying of γ.

(**a**)
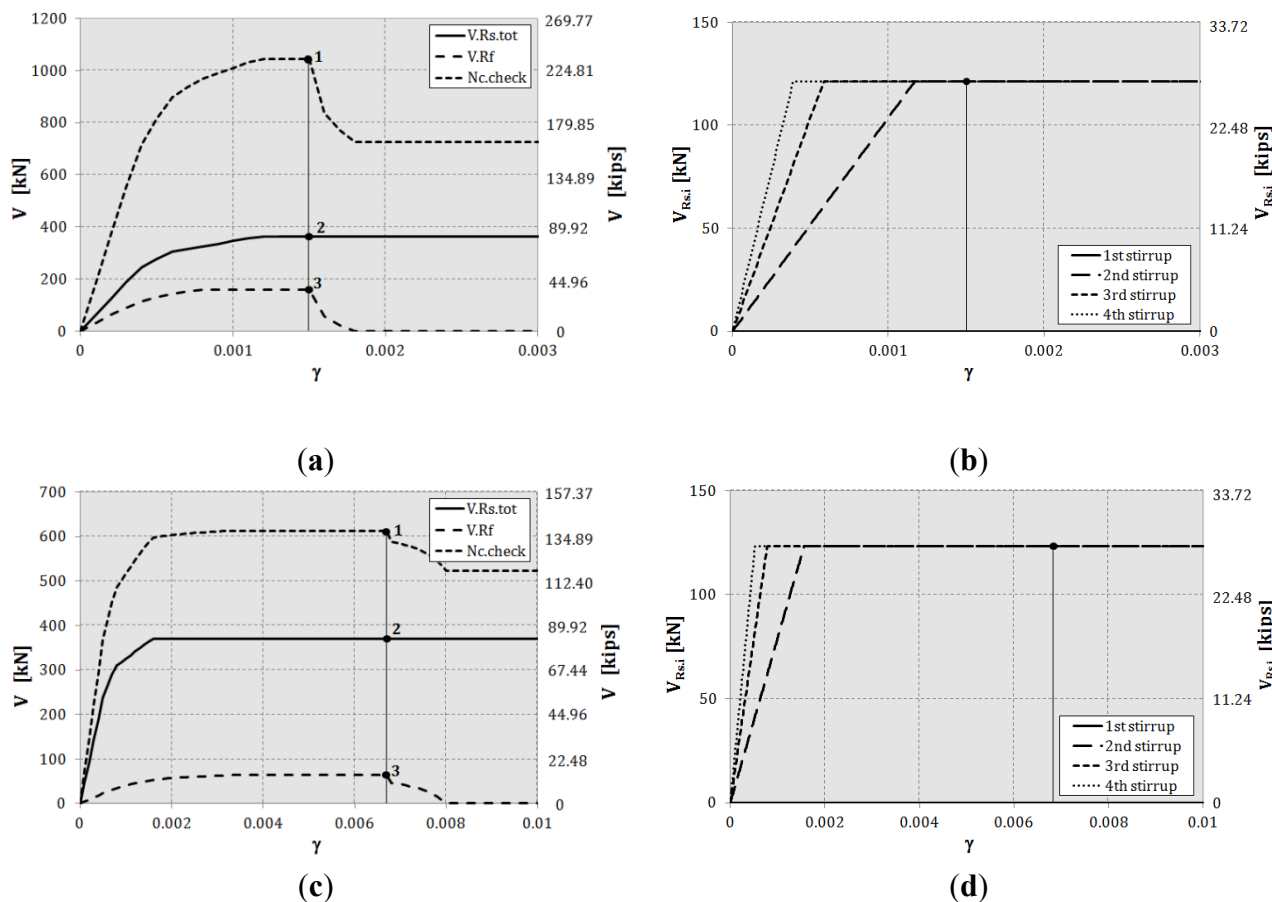

(**b**)

(**c**)

(**d**)

Figure 9a–c demonstrates that for some combinations of parameters (see Table 2), the concrete strut crushes before the FRP sheet debonds and the stirrups yield: in fact, referring to (a), at $\gamma \approx 0.0003$, the short-dotted curve representing the axial force acting in the concrete drops to zero, meaning that the concrete crushes. At this point, the FRP sheet has not yet reached the maximum resisting value, and among the eight stirrups intercepted by the crack (see (b)), three are yielded and five are still elastic, contributing to the shear capacity proportionally to their real stress; see Equation (4).

Figure 10a–c and Table 3 refer to the case of an FRP sheet that debonds before all of the stirrups yielded: with reference to (a), at $\gamma \approx 0.0022$, the FRP sheet reaches its maximum capacity, four stirrups are yielded and one stirrup, which is closest to the crack tip, is still elastic; see (b) and Figure 3.

Table 2. Crushing of concrete: parameters.

Case	H (mm)	θ (degrees)	s (mm)	E_f (GPa)	E_s (GPa)	t_f (mm)	t	R_{ck} (MPa)	f_{yk} (MPa)	α_s (degrees)	ϕ_s (mm)
(a) (c)	600	30	100	390	210	0.44 0.254	1 0.5	18	335	90	8

Figure 9. Crushing of concrete: (**a**,**c**) the contribution of FRP and stirrups to the shear capacity at varying of γ; (**b**) the actual contribution of each stirrup at varying of γ.
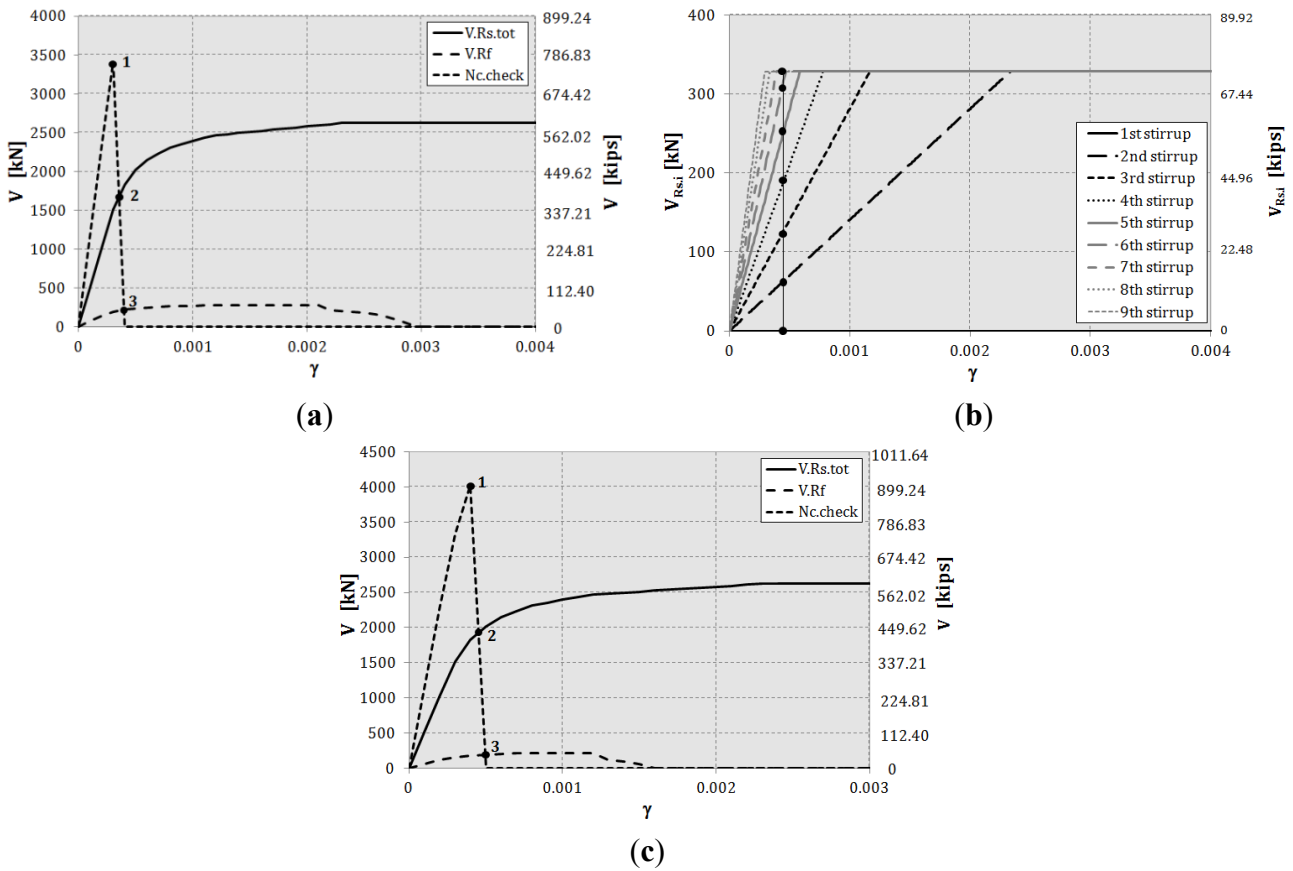

(a)

(b)

(c)

Table 3. Debonding of FRP sheet.

Case	H (mm)	θ (degrees)	s (mm)	E_f (GPa)	E_s (GPa)	t_f (mm)	t	R_{ck} (MPa)	f_{yk} (MPa)	α_s (degrees)	ϕ_s (mm)
(a)	400	30									8
(c)	500	36	100	390	210	0.254	1	30	430	90	10

Figure 10. FRP debonding: (**a**,**c**) the contribution of FRP and stirrups to the shear capacity at varying of γ; (**b**,**d**) the actual contribution of each stirrup at varying of γ.
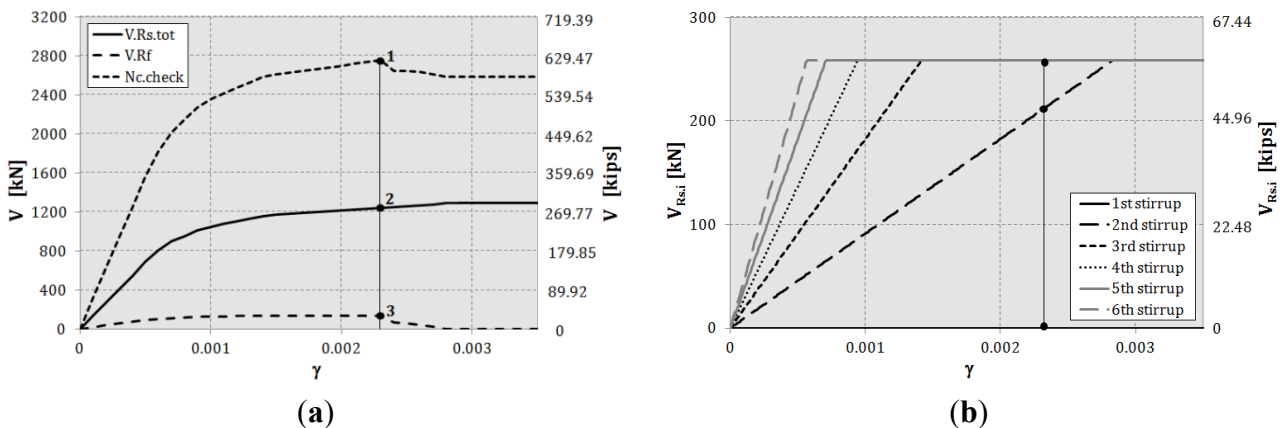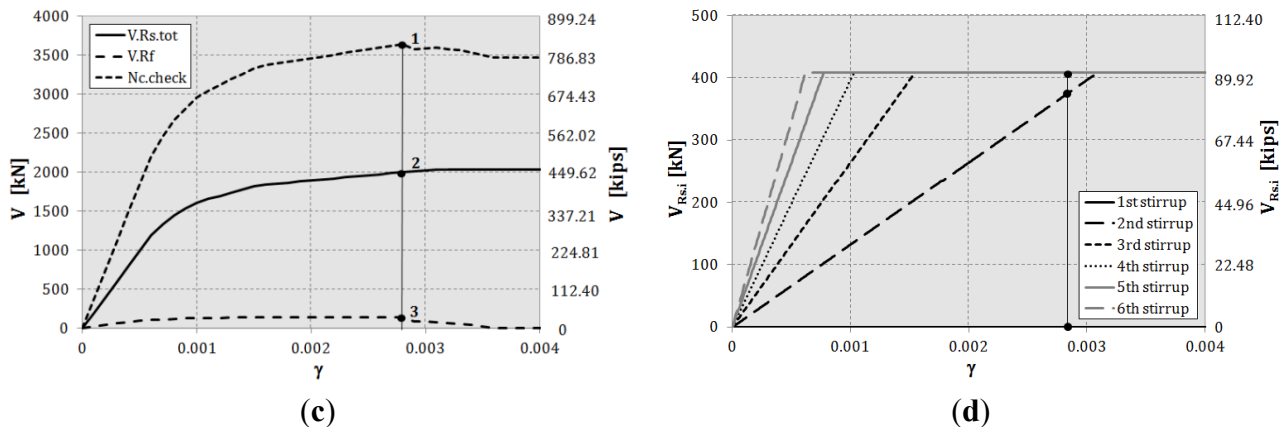

(a)

(b)

Figure 10. *Cont.*

(c)

(d)

These last two cases demonstrate that the common accepted rule of assuming the shear capacity of FRP-RC beams in shear as the sum of the maximum contribution of both FRP and stirrups can lead to an unsafe overestimation of the actual shear capacity.

8. Validation of the Model against Experimental Results

For the purpose of validating the capability of the proposed model to estimate the shear strength of FRP-RC members, a comparison between experimental results and model predictions has been carried out.

Very few tests have been found in the literature to be taken as a reliable benchmark to validate the model, since most of those available do not report all of the information required to check the model.

As for the comparative study shown hereafter, experimental data have been gathered from an experimental campaign conducted by Grande *et al.* [15], referring only to those reporting all of the measurements necessary to verify the model.

Table 4 summarizes the geometry and materials of the three considered RC beams, strengthened in shear with FRP sheets and subjected to a three-point flexural test: basically, the specimens differ from each other for the stirrups spacing, *s,* and the inclination of the main crack at the end of the test, θ.

Table 4. Specimens: geometry and materials.

Sample	H (mm)	b_w (mm)	θ (degrees)	s (mm)	E_f (GPa)	E_s (GPa)	t_f (mm)	t	R_{ck} (MPa)	f_{yk} (MPa)	α_s (degrees)	ϕ_s (mm)
1			30	200								
2	450	250	20	300	392	210	0.191	1	25	650	90	8
3			24	400								

In Table 5, the comparison between the experimental results and the predictions of the model is shown in terms of the contribution of FRP sheets to the shear strength and total shear strength, both explicitly provided in the paper. The contribution of the stirrups, which is not given, has been calculated by imposing the compatibility condition along the crack, expressed by Equation (4).

The accuracy of the model has been evaluated referring to the overall shear capacity: the comparison demonstrates that the proposed model is able to predict the shear capacity of the FRP-RC beams with an error less than 10%.

Table 5. Comparison: experimental results and model predictions.

Sample	V_{Rf} (kN)		$V_{Rs.tot}$ (kN)		Total shear force (kN)		
	Experiment	Model	Experiment	Model	Experiment	Model	Error (%)
1	65	71		191	280	262	**6**
2	110	110	–	145	270	255	**5**
3	100	107		97	225	204	**9**

The three tests here considered, even though in a limited number, yield very promising results. Hopefully, with more experimental campaigns being carried out in recent years, in the future, there will be more comprehensive data available to completely validate the proposed model.

9. Conclusions

This work goes along the theoretical line traced by Monti and Liotta [6], whereby the stress state in an FRP-shear-strengthened reinforced concrete element is accurately followed, with particular reference to the transverse steel stirrups, the strengthening FRP sheet/strips and the concrete strut, by progressively widening a shear crack that crosses them. This allows computing at any crack width the contributions from steel and FRP, while checking that the compressed concrete is not crushed, and correctly evaluating the evolution of the shear capacity at any step. In particular, the model allows one to verify whether the steel stirrups are yielded (either all or some of them) when FRP debonds. The objective is that of verifying if the usual assumption of adding the steel and FRP contribution is a meaningful one, also in view of the fact that it helps with simplifying the design equations. What has been observed, instead, is that there are (not peculiar) situations where the steel stirrups are still elastic when the FRP debonds: in those conditions, the actual shear capacity is lower than that computed through the purely additive formulas. This demonstrates that the current design equations need to be adjusted to account for this occurrence, which is the objective of ongoing research work.

Acknowledgments

Conflicts of Interest

The authors declare no conflict of interest.

References

1. *Building Code Requirements for Structural Concrete and Commentary*; ACI Committee 318; American Concrete Institute (ACI): Farmington Hills, MI, USA, 2008.

2. *Instructions for Design, Execution and Control of Strengthening Interventions Through Fiber-Reinforced Composites*; CNR-DT 200 R1/2013; Consiglio Nazionale delle Ricerche (CNR): Rome, Italy, 2014.

3. Lima, J.; Barros, J. Reliability analysis of shear strengthening externally bonded FRP models. *Proc. Inst. Civ. Eng. Struct. Build.* **2011**, *164*, 43–56.

4. Khalifa, A.; Gold, W.J.; Nanni, A.; Aziz, A.M.I. Contribution of externally bonded FRP to shear capacity of RC flexural members. *ASCE J. Compos. Constr.* **1998**, *2*, 195–202.

5. Triantafillou, T.C.; Antonopoulos, C.P. Design of concrete flexural members strengthened in shear with FRP. *J. Compos. Constr.* **2000**, *4*, 198–205.

6. Chen, J.F.; Teng, J.G. Shear capacity of FRP-strengthened RC beams: FRP debonding. *Constr. Build. Mater.* **2003**, *17*, 27–41.

7. Carolin, A.; Taljsten, B. Theoretical study on strengthening for increased shear bearing capacity. *J. Compos. Constr.* **2005**, *9*, 497–506.

8. Monti, G.; Liotta, M. Tests and design equations for FRP-strengthening in shear. *Constr. Build. Mater.* **2007**, *21*, 799–809.

9. Chaallal, O.; Shahawy, M.; Hassan, M. Performance of reinforced concrete T-girders strengthened in shear with CFRP fabrics. *ACI Struct. J.* **2002**, *99*, 335–343.

10. Pellegrino, C.; Modena, C. An experimentally based analytical model for shear capacity of FRP strengthened reinforced concrete beams. *Mech. Compos. Mater.* **2008**, *44*, 231–244.

11. Bukhari, I.A.; Vollum, R.L.; Ahmad, S.; Sagaseta, J. Shear strengthening of reinforced concrete. *Mag. Concr. Res.* **2010**, *62*, 65–77.

12. *Eurocode 2: Design of Concrete Structures—Part 1-1: General Rules and Rules for Buildings*; EN 1992–1-1; The European Committee for Standardization (CEN): Milano, Italy, 2005.

13. Mofidi, A.; Chaallal, O. Shear strengthening of RC beams with EB FRP: Influencing factors and conceptual debonding model. *J. Compos. Constr.* **2011**, *15*, 62–74.

14. Regan, P.E. Research on shear: A benefit to humanity or a waste of time? *Struct. Eng.* **1993**, *71*, 337–347.

15. Grande, E.; Imbimbo, M.; Rasulo, A. Experimental response of RC beams strengthened in shear by FRP sheets. *Open Civ. Eng. J.* **2013**, *7*, 126–134.